ENVIRONMENTAL RESEARCH
LETTERS

LETTER • OPEN ACCESS

Model consistency for the underlying mechanisms for the Inter-decadal Pacific Oscillation-tropical Atlantic connection

ENVIRONMENTAL RESEARCH
LETTERS

LETTER

Model consistency for the underlying mechanisms for the Inter-decadal Pacific Oscillation-tropical Atlantic connection

Shuai-Lei Yao[1,*], **Pao-Shin Chu**[2], **Renguang Wu**[3] **and Fei Zheng**[4,5]

[1] State Key Laboratory of Numerical Modeling for Atmospheric Sciences and Geophysical Fluid Dynamics, Institute of Atmospheric Physics, Chinese Academy of Sciences, Beijing 100029, People's Republic of China
[2] Department of Atmospheric Sciences, School of Ocean and Earth Science and Technology, University of Hawai'i at Mānoa, Honolulu, HI 96822, United States of America
[3] School of Earth Sciences, Zhejiang University, Hangzhou 310027, People's Republic of China
[4] School of Atmospheric Sciences, Key Laboratory of Tropical Atmosphere-Ocean System, Ministry of Education, Sun Yat-sen University, Zhuhai, People's Republic of China
[5] Southern Marine Science and Engineering Guangdong Laboratory, Zhuhai 519082, People's Republic of China
[*] Author to whom any correspondence should be addressed.

E-mail: yaoshl08@hotmail.com

Keywords: Inter-decadal Pacific Oscillation, tropospheric temperature warming mechanism, water vapor-longwave radiation-SST positive feedback, trans-basin Pacific-Atlantic teleconnection

Supplementary material for this article is available online

OPEN ACCESS

RECEIVED
7 September 2022

REVISED
27 October 2022

ACCEPTED FOR PUBLICATION
15 November 2022

PUBLISHED
23 November 2022

Abstract

Modeling evidence suggests that the Inter-decadal Pacific Oscillation (IPO) can remotely affect the tropical Atlantic sea surface temperature (SST) variability. However, the root causes of the IPO-tropical Atlantic inter-basin teleconnections are not fully understood. Using idealized pacemaker experiments wherein the observed IPO-SST anomalies are specified, we show that a warm-phase IPO-SST anomaly drives a basin-wide SST warming over the tropical Atlantic. The trans-basin IPO-tropical Atlantic connection is established via the tropical tropospheric temperature mechanism and the atmospheric bridge teleconnections. An IPO positive-phase SST initiates the warming tropospheric temperature anomalies, leading to a more humid atmosphere and increasing longwave radiation downward into the tropical Atlantic. By comparison, the reduced Pacific Walker circulation and mid-latitude Rossby wave responses cause the trade winds to strengthen, acting to suppress the tropical Atlantic warming through the Bjerknes positive feedback mechanism. Thus, similar to previous studies, the tropical Atlantic widespread warming is ultimately traced back to the warming effects generated by the water vapor-longwave radiation-SST positive feedback, which, contrary to previous studies, overwhelms the cooling effects associated with the intensified trade winds. Our results highlight the model dependence on the details of mechanisms that connect the tropical Pacific and tropical Atlantic on the decadal timescales.

1. Introduction

Modeling and observational evidence suggest that the Pacific sea surface temperature (SST) variations substantially influence the tropical Atlantic Ocean, affecting its inter-annual and decadal timescale variability (Chang *et al* 2006b, Cai *et al* 2019). The Atlantic SST variability modulates the global climate system, with widespread climatic consequences. For example, anomalous warming over the north tropical Atlantic drives a northward swing of the Atlantic inter-tropical convergence zone (Chang *et al* 2000), thus causing droughts in Northeast Brazil and central-eastern Amazon (Hastenrath and Heller 1977), as well as floods across northern South America and Caribbean regions (Grimm and Tedeschi 2009). The north tropical Atlantic warming also induces increasing risks of landfall hurricane frequency in the U.S. (Xie *et al* 2005), triggers the central Pacific La Niña events (Ham *et al* 2013), and influences the Antarctic sea ice redistribution (Li *et al* 2014, 2021). Thus, determining the potential mechanisms for the trans-basin Pacific-Atlantic connections is societally essential.

The tropical Pacific-Atlantic teleconnections have been well established on the inter-annual timescale. The El Niño-Southern Oscillation (ENSO), the most noticeable year-to-year variation on Earth, originates in the tropical Pacific and alternates between warm El Niño and cold La Niña events. After an El Niño matures, the north tropical Atlantic typically warms for a few months during the boreal spring and early summer (Chiang and Sobel 2002, Kumar and Hoerling 2003, Taschetto *et al* 2016) as a consequence of reduced surface latent heat flux associated with the weakened northeasterly winds via the atmospheric bridge teleconnections (Klein *et al* 1999) or the dampened moist convection and circulation via the tropospheric temperature mechanism (Chiang and Sobel 2002). The Pacific El Niño-like warming also impacts the equatorial and south tropical Atlantic, and the associated responses are relatively weak. Specifically, an El Niño event produces a reduced Pacific Walker circulation and strengthened trade winds in and to the south of the equatorial Atlantic (Chiang and Sobel 2002, Sasaki *et al* 2015), inducing cold SST anomalies along the equator and to the south of the tropical Atlantic during the boreal spring and summer through Bjerknes feedback (Bjerknes 1969) that may counter the tropospheric temperature warming response (Chang *et al* 2006a). Thus, warm or neutral conditions may occur in the equatorial and south tropical Atlantic.

On the decadal timescales, the physical processes for the trans-basin Pacific–Atlantic teleconnections remain controversial (Latif 2001). The Interdecadal Pacific Oscillation (IPO), sometimes also called Pacific Decadal Oscillation (Power *et al* 1999, Newman *et al* 2016), emerges as the leading Empirical Orthogonal Function mode of Pacific decadal SST variability after the radiatively forced component has been subtracted at each grid point (Zhang *et al* 1997). Observations document the inter-basin Pacific-Atlantic links in decadal SST variability (Nigam *et al* 2020), with the warm tropical Pacific leading with the same sign in the tropical Atlantic by ∼three years (Meehl *et al* 2021), despite the lack of the involved mechanisms due to the limited instrument records. Modeling studies show that a warm-polarity IPO SST forces anomalous warming in the tropical Atlantic through the Walker circulation perturbations and mid-latitude atmospheric Rossby wave responses (Meehl *et al* 2021). However, little is known about whether the proposed mechanisms are model-dependent. Less appreciated is which underlying mechanism is largely responsible for the IPO-tropical Atlantic connections.

Here, we revisit a recent study of CESM1 (Meehl *et al* 2021) and analyze similar idealized Pacific pacemaker experiments with two additional coupled models to investigate the model dependence on the tropical Pacific-Atlantic connections. Our study confirms that an IPO warm-phase SST drives the basin-wide decadal SST warming in the tropical Atlantic via a tropical troposphere temperature-induced surface heat flux mechanism. We also demonstrate for these two models that the proposed mechanism overwhelms latent heat flux reduction related to the enhanced trade winds over the tropical Atlantic.

2. Methods and experimental setup

To illuminate how a warm-phase IPO-SST anomaly affects the tropical Atlantic climate anomalies, we evaluate idealized IPO pacemaker simulations with only two current coupled models, including IPSL-CM6A-LR and HadGEM3-GC31-MM, wherein a time-invariant spatial pattern corresponding to the internally-generated component of observed IPO-SST anomalies is constrained, as a contribution to the Decadal Climate Prediction Project (Boer *et al* 2016). The atmospheric component of IPSL-CM6A-LR has 144 × 143 longitude/latitude and 79 vertical layers with a ∼80 km top-level. Its ocean model has a quasi-isotropic tripolar grid of 1° nominal resolution and 75 ocean levels (Boucher *et al* 2020). HadGEM3-GC31-MM has a high-resolution atmospheric component of 432 × 324 longitude/latitude and 85 vertical layers with a ∼85 km top-level, together with an oceanic component having a tripolar grid of ∼0.25° and 75° ocean levels (Roberts *et al* 2019). Both models reasonably reproduce the characteristics of ENSO and IPO, despite common mean-state SST biases (Roberts *et al* 2019, Boucher *et al* 2020).

The IPO index and its SST pattern utilized in idealized pacemaker simulations are calculated from the observed SST from 1900 to 2013 (ERSST V4). Following earlier approaches (Ting *et al* 2009, Ruprich-Robert *et al* 2017, Meehl *et al* 2021, Yao *et al* 2021), the externally-forced SST response is first taken from the CMIP5 multi-model ensemble under historical simulations (1870–2005) and Representative Concentration Pathway 8.5 (RCP8.5; 2006–2013) and then removed from observations. Finally, the IPO index is estimated as the leading principal component of an empirical orthogonal function decomposition to the observed residual SST over the Pacific domain (40°S–60°N, from Indonesia to the American Coast). The IPO-SST spatial pattern is obtained by regressing the IPO index onto SSTs at each grid point from 1900 to 2013 (figure S1).

The Pacific-wide SSTs are restored to an IPO-SST spatial pattern in these two global coupled models by adding the non-solar surface heat fluxes to the mixed layer (Haney 1971, Frankignoul and Kestenare 2002, Servonnat *et al* 2015). Here, the heat flux adjustments are made following the restoring term:

$$F = \frac{dQ}{dT}(SST_{model} - SST_{target})$$

where $\frac{dQ}{dT}$ is a constant restoring coefficient of -40 W m^{-2} K^{-1} corresponding to a restoring timescale of approximately 60 days for a 50 m-depth mixed layer. Outside the targeted region, SSTs are free to evolve and are coupled to the overlying atmosphere.

Table S1 outlines two sets of 10-member and 25-member ensemble experiments of IPSL-CM6A-LR and HadGEM3-GC31-MM for the idealized IPO pacemaker configurations. In the full IPO pacemaker simulations, an IPO-SST anomaly pattern of positive-polarity and negative-polarity is separately prescribed over the Pacific domain (40°S–60°N and from Indonesia to the American Coast in figure S1(a)), hereafter denoted as IPO+ and IPO−. In the North IPO simulations (called Nor_IPO+ and Nor_IPO−), similar to the IPO+ and IPO− but only the northern part of IPO is specified from 20°N to 60°N (figure S1(b)), which approximately represents a Pacific Decadal Oscillation (PDO)-SST anomaly (Newman *et al* 2016). These two distinctive pacemaker experiments aim to gain insight into the relative importance of IPO and PDO in driving the trans-basin Pacific-Atlantic teleconnections. All radiative forcing agents are kept constant at the pre-industrial levels in each experiment. Each realization is run for only ten-model years to avoid creating climate anomalies over the unrestored subsurface ocean caused by deep ocean circulation that could deteriorate the tropical Atlantic climate response to the IPO SST forcing. We assume the linearity of the Atlantic climate response to the warm-phase and cold-phase IPO and directly examine the consequence of a negative-to-positive phase transition of IPO (disregarding a neutral state). To maximize the signal-to-noise ratio, we extract the Atlantic climate response to a warm-phase IPO-SST forcing by taking the difference between IPO+ and IPO− ensemble simulations rather than comparing the perturbation experiments to a control run. The results presented here are calculated from the ensemble mean of each model experiment. In this study, we analyze each year of the individual ensemble realizations to evaluate the statistical significance of the difference between IPO+ (North_IPO+) and IPO− (North_IPO−) using the two-sided Student *t*-test.

3. Results

3.1. The potential impact of an IPO-SST anomaly on the Atlantic climate change

Figure 1 exhibits the Atlantic decadal-timescale climate response to the full and North IPO-SST anomalies. For the full IPO warm-polarity case (IPO+ minus IPO−), most of the tropical Pacific is characterized by significant warm SST anomalies of over 0.4 °C (figures 1(a) and (b)), comparable to the observed SST (figure S1). Both models consistently simulate the widespread warm SST anomalies over the tropical Atlantic, with a stronger magnitude in HadGEM3-GC31-MM (0.2 °C–0.4 °C) than IPSL-CM6A-LR (0.1 °C–0.2 °C). Correspondingly, anomalous westerly surface winds appear over the central-western equatorial Pacific, while easterly surface wind anomalies occupy the far-eastern Pacific, tropical Atlantic, and the equatorial Indian Oceans. Alternating anomalous cyclones and anti-cyclones extend from the North Pacific to North America and South Pacific to the Amundsen Sea, ending with anomalous anti-cyclones centered over the North and South tropical Atlantic, respectively. Unlike the full IPO-SST forcing (figures 1(a) and (b)), a North IPO-SST warming, representing a warm-phase PDO, forces relatively weak warm SST anomalies and reduced trade winds over the tropical Atlantic (figures 1(c) and (d)). We note that an anomalous anti-cyclone is seen over the North Atlantic, in contrast to an anomalous cyclone resulting from a full IPO warm-phase SST forcing. The results suggest that a full IPO warm-phase SST, particularly in the tropical domain that plays a major role (Deser *et al* 2004), significantly drives the decadal-scale climate anomalies in the tropical Atlantic.

Although the IPO and PDO indices are highly correlated ($r = \sim$0.9 with >95% significance) in observations (Han *et al* 2014), their respective global influences in coupled models are distinctive. Compared to a cold-phase PDO (Nor_IPO− minus Nor_IPO+ in figure S2), an IPO-SST cooling forces stronger surface easterly wind anomalies over the tropical Pacific and larger cold SST anomalies worldwide, supporting the notion of a cold-phase IPO dominating the early-2000s hiatus (Kosaka and Xie 2013, Meehl *et al* 2016). As corroborated by recent findings (Meehl *et al* 2021), an IPO-SST anomaly triggers a basin-wide SST response across the tropical Atlantic on the decadal timescale, with comparable magnitude in the same sign as the tropical Pacific. In contrast, a warm tropical North Atlantic typically follows an El Niño event on the interannual timescale (Curtis and Hastenrath 1995). Therefore, we aim to provide helpful insight into the potential mechanisms for a warm-phase IPO-SST anomaly exciting the tropical Atlantic basin-scale warming.

3.2. Tropical and extra-tropical dynamical pathways for affecting the tropical Atlantic climate response

We explore the respective roles of the tropical and extra-tropical atmospheric teleconnections in relaying the warm-polarity IPO-SST signal to the tropical Atlantic. The atmospheric baroclinic vertical structure in the tropics is estimated by half the difference between stream functions at 850 hPa and 200 hPa

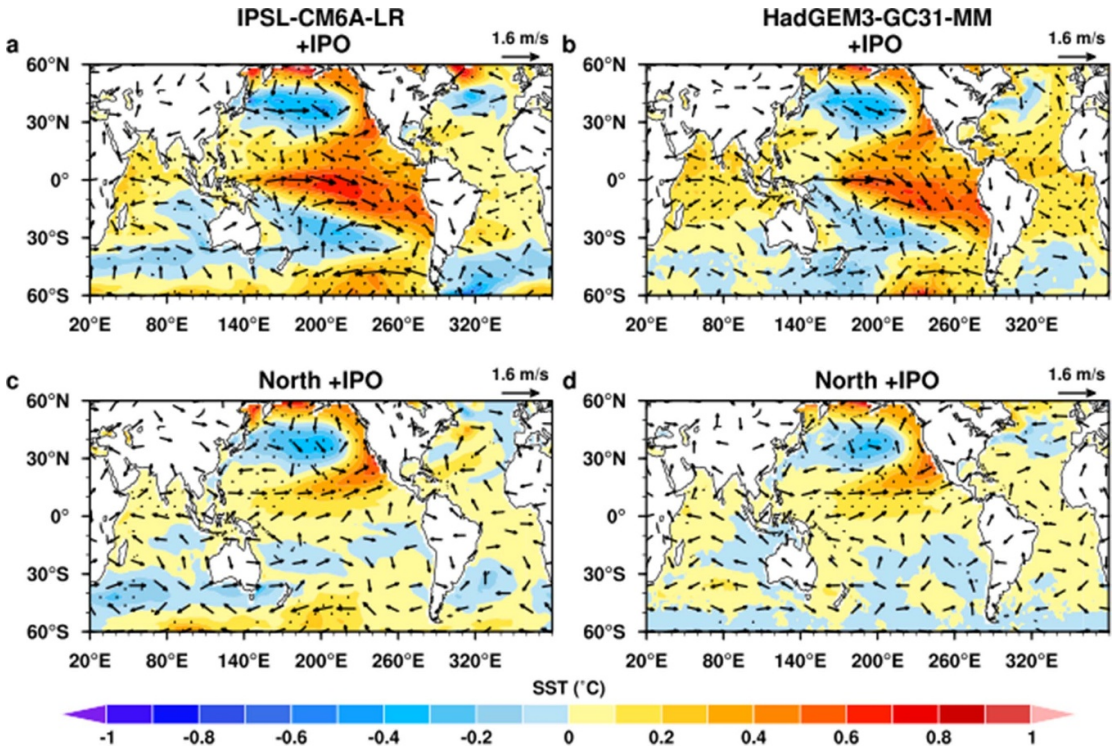

Figure 1. The Atlantic decadal-scale climate response to the Interdecadal Pacific Oscillation (IPO) warm-phase SST anomaly in IPSL-CM6A-LR (left panel) and HadGEM3-GC31-MM (right panel). Ten-year ensemble mean of SST (shading) and 850 hPa winds (arrows with the key at the top right) for (a), (b) IPO+ minus IPO− (denoted +IPO), and for (c), (d) Nor_IPO+ minus Nor_IPO− (denoted North +IPO). Stippling denotes regions that are statistically significant above a 95% confidence level based on a two-sided Student's *t*-test.

levels (Yu *et al* 2010). An IPO-SST warming drives a southward shift of the North Pacific intertropical convergence zone and a northeastward shift of the South Pacific convergence zone (figures 2(a) and (b)), accompanied by an enhanced ascending motion over the equatorial eastern Pacific and a reduced Pacific Walker circulation (figures 2(c) and (d)). The associated convective heating anomalies in the tropical eastern Pacific excite a baroclinic atmospheric response within the tropics, characterized by a pair of baroclinic cyclones straddling the equatorial Pacific and another pair of baroclinic anti-cyclones covering the tropical Atlantic and tropical Indian Oceans. This circulation pattern resembles a typical Gill–Matsuno response (Gill 1980), as expected from the composite four-season evolutions of ten-year idealized pacemaker simulations in both models (figures S3 and S4). In the January–February–March, the eastern Pacific warming-driven atmospheric deep convection initiates an equatorial Kelvin wave, generating easterly surface wind anomalies across the equatorial Atlantic and Indian Oceans, as well as Rossby wave packets associated with equatorial westerly wind anomalies over the western Pacific. From April–May–June to July–August–September, the eastern Pacific convection activity enhances and shifts westward toward the International Dateline. By October–November–December, the prescribed warm-phase IPO SST anomaly eventually coexists with the basin-wide warm SST in the tropical Atlantic.

Additionally, in response to a warm-polarity IPO SST anomaly, significant tropospheric temperature warming occurs the entire tropical free troposphere (figures 2(e) and (f)), as measured by the column-integrated tropospheric atmospheric temperature anomalies from 1000 hPa to 200 hPa. More overlooked, however, is that the tropospheric temperature significant warming in the tropical eastern Pacific is almost in phase with coherent warming across the tropical Atlantic and Indian oceans. By comparing the composited four-season evolutions of column-integrated tropospheric temperature anomalies from the ten-year idealized pacemaker simulations (figure S5), it is clear that the magnitude of the tropospheric temperature response over the tropical Atlantic and Indian Oceans is more dependent on the tropospheric atmospheric temperature warming anomalies over the tropical eastern Pacific. These results identify the predominance of an IPO warm-phase SST over the tropospheric atmospheric temperature warming on the decadal timescales, in close agreement with earlier findings of the ENSO mediating the inter-annual tropospheric temperature variability across the tropical Oceans (Pan and Oort 1983, Yulaeva and Wallace 1994, Soden 2000).

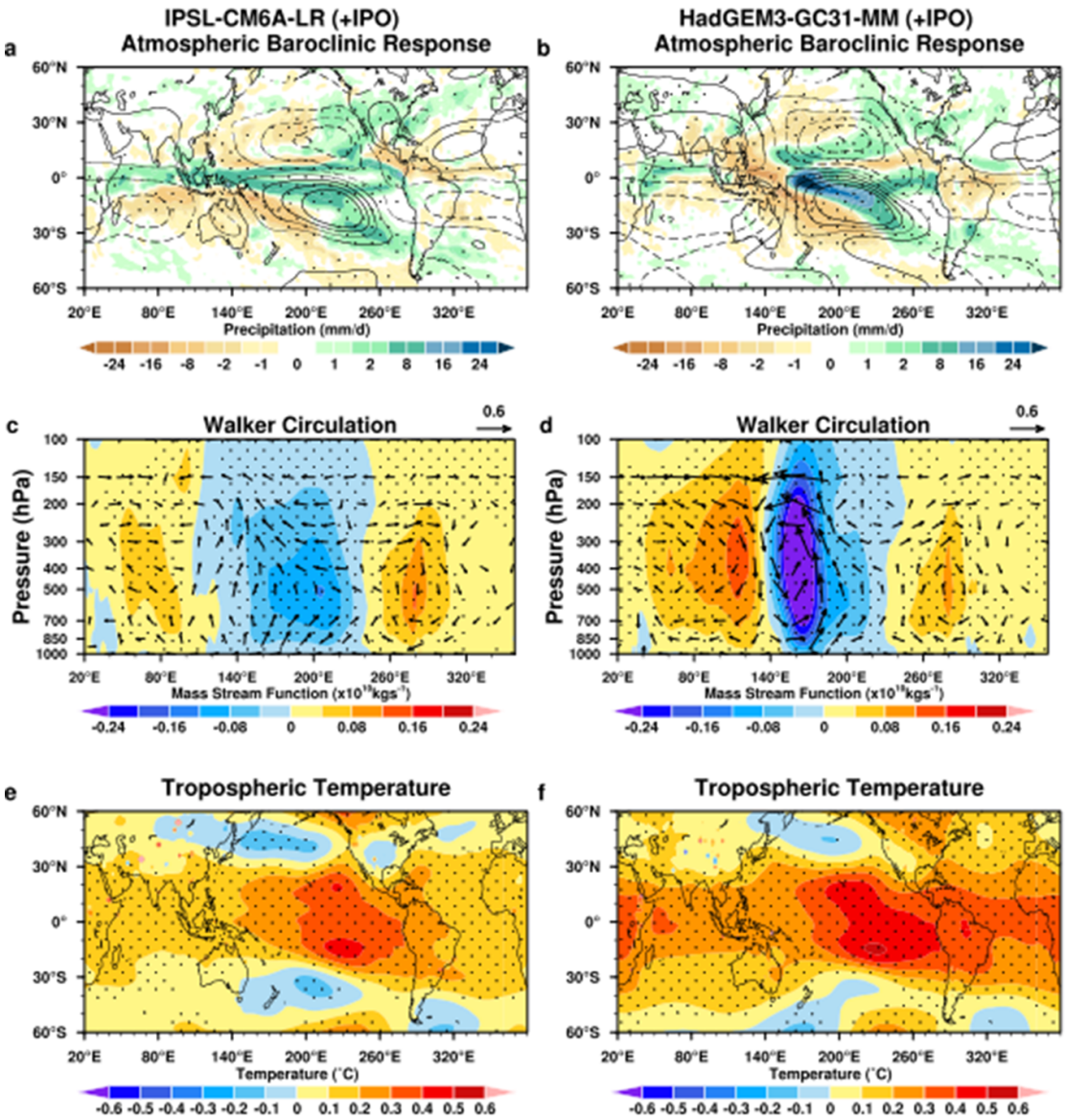

Figure 2. Tropical pathway for a warm-phase IPO-SST anomaly driving tropical Atlantic response in IPSL-CM6A-LR (left panel) and HadGEM3-GC31-MM (right panel) for IPO+ minus IPO−. (a), (b) Precipitation (shading) and atmospheric baroclinic response (contours with interval of 0.4×10^6 kg^{-1} from -1.4×10^6 kg^{-1} to 1.4×10^6 kg^{-1}; solid and dashed contours denote positive and negative values, respectively). The atmospheric baroclinic response is estimated as half difference between the 850 hPa stream function and 200 hPa stream function. Note that the zonal mean of atmospheric baroclinic response has been subtracted. (c), (d) Zonal mass stream function (shading; overlying vectors represent divergent zonal wind and vertical velocity scaled by a factor of −25). Negative (positive) values indicate an anti-clockwise (clockwise) rotation and, thus, a weakened (enhanced) Walker circulation. The zonal mass stream function is computed by vertically integrating the meridionally-averaged component (between 5°S and 5°N) of divergent zonal wind from the top-level downward. (e), (f) The column-integrated tropospheric temperature changes from 1000 hPa to 200 hPa. Stippling, black contours, and vectors denote statistically significant regions above a 95% confidence level based on a two-sided Student's *t*-test.

In addition to the tropical atmospheric teleconnections, a positive-phase IPO-SST anomaly can also remotely influence the North and South Atlantic via the mid-latitude atmospheric teleconnections. An IPO-SST warming yields positive precipitation anomalies and the enhanced latent heat release over the tropical eastern Pacific (figures 2(a) and (b)), subsequently heating the overlying atmosphere and triggering a two-pronged, large-scale Rossby wave train (figures 3(a) and (b)). This Rossby wave response first extends from the tropical Pacific to the North and South Pacific, then propagates eastward, and ultimately reaches the North and South Atlantic, respectively. The composite seasonal evolutions of the wave activity flux for the ten-year idealized pacemaker simulations provide strong support for the mid-latitude Rossby wave response (Takaya and Nakamura 2001) from 30°N to 80°N in the North Hemisphere and from 30°S to 80°S in the South Hemisphere (figure S6). These alternating active low-pressure and high-pressure centers bear a striking resemblance to an anomalous Pacific-North America pattern to

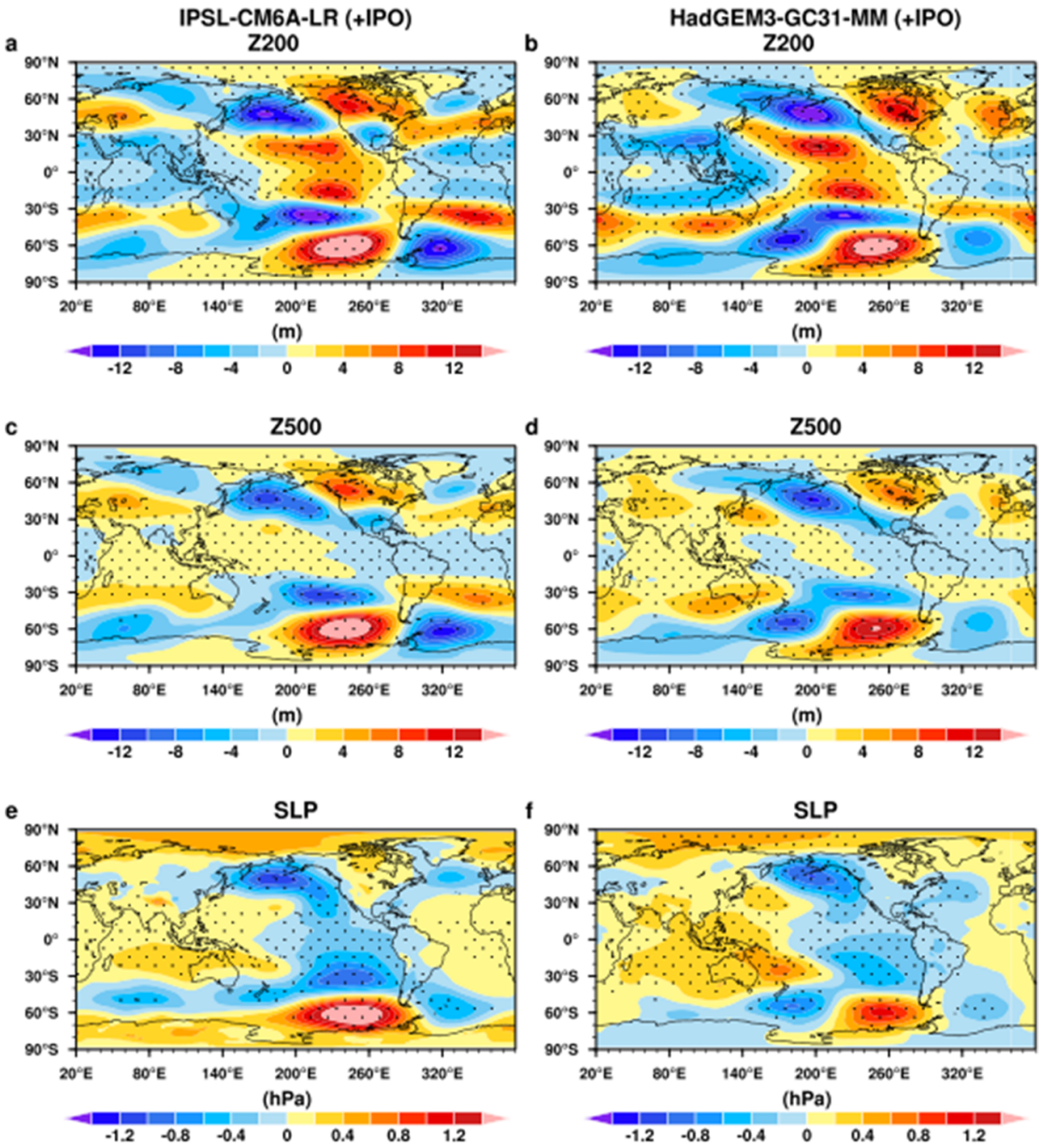

Figure 3. Extra-tropical pathway for an IPO-SST warming anomaly driving the Atlantic circulation change in IPSL-CM6A-LR (left panel) and HadGEM3-GC31-MM (right panel) for IPO+ minus IPO−. (a), (b) 200 hPa geopotential height with zonal mean removed (Z200), (c), (d) 500 hPa geopotential height with zonal mean removed (Z500), and (e), (f) sea level pressure (SLP). Stippling denotes regions exceeding 95% statistical significance based on a two-sided student *t*-test.

the north and east (Wallace and Gutzler 1981) and an anomalous Pacific-South America Pattern to the south and east (Mo 2000), each with highly equivalent barotropic structures with amplitude from sea level to mid-troposphere (500 hPa) and even up to 200 hPa ending with low center anomalies in the extra-tropical North and South Atlantic (figure 3).

As a result, increased sea level pressure is seen over the tropical Atlantic (figures 3(e) and (f)), inducing an enhanced zonal pressure gradient between the tropical Atlantic-tropical eastern Pacific and thus favoring intensified trade winds over the tropical Atlantic. The strengthened easterly winds are conducive to SST cooling over the tropical Atlantic via the Bjerknes feedback mechanism (Bjerknes 1969), in contrast to the tropospheric temperature warming mechanism. Note that the tropical Atlantic easterly wind strength relies largely on the location of low-pressure anomalies over the extra-tropical Atlantic. Due to a farther poleward position of anomalous low-pressure active centers in the extra-tropical North and South Atlantic in IPSL-CM6A-LR (located near 50°N and 65°S in figure 3(e)) than HadGEM3-GC31-MM (located near 30°N and 50°S in figure 3(f)) and CESM1 (located near 30°N and 50°S in figure S4(a) of Meehl *et al* 2021), intensified trade winds occupy most of the tropical Atlantic in the former (c.f. figures 1(a) and (b)), while relatively weak easterlies only occur near the equatorial Atlantic in the last two models.

To better understand the role of a warm-phase IPO-SST anomaly in determining the trans-basin Pacific-Atlantic connection, we further evaluate the contributions of a PDO positive-phase SST anomaly to generate tropical and mid-latitude atmospheric teleconnections. We found that a PDO-SST forcing exerts a marginal impact on the tropospheric atmospheric temperature warming (figure S7) and mid-latitude Rossby wave responses (figure S8). The distinctive tropical Atlantic decadal SST responses to the warm-polarity IPO-SST and PDO-SST anomalies in both models emphasize the importance of an IPO-SST warming in triggering the tropical Pacific-tropical Atlantic decadal teleconnections.

3.3. Potential mechanisms for a warm-phase IPO-SST driving the tropical Atlantic warming

A positive-polarity IPO-SST anomaly linkage to the tropical Atlantic on the decadal timescale has been successfully established via the tropical and mid-latitude atmospheric teleconnections in two global coupled models and discussed in the context of earlier comparable results from a third coupled model (Meehl *et al* 2021). We investigate in more detail the major driver for a warm-phase IPO-SST anomaly leading to basin-wide decadal warming in the tropical Atlantic. Following earlier studies (Xie *et al* 2010, Yao *et al* 2021), the ocean mixed-layer heat-budget analysis is expressed as:

$$\frac{\partial T}{\partial t} = \frac{1}{C_p^o \rho_o H}\left(Q_L + Q_S + \frac{\overline{Q_E}}{e^{\alpha\overline{\Delta T}} - \overline{RH}}RH' + \frac{\alpha\overline{Q_E}\,\overline{RH}}{e^{\alpha\overline{\Delta T}} - \overline{RH}}\Delta T' + \frac{\overline{Q_E}}{\overline{W}}W' + Q_H + D_o + \text{Residual}\right)$$

where T, c_p^o, ρ_o, and H are SST, the specific heat at constant pressure, the density of seawater, and the mixed-layer depth (a constant 50 m), respectively. The heat-budget terms on the right-hand side of the equation encapsulate longwave radiation (Q_L), shortwave radiation (Q_S), latent heat flux due to changes in near-surface relative humidity ($\frac{\overline{Q_E}}{e^{\alpha\overline{\Delta T}} - \overline{RH}}RH'$), changes in surface atmospheric stability ($\frac{\alpha\overline{Q_E}\,\overline{RH}}{e^{\alpha\overline{\Delta T}} - \overline{RH}}\Delta T'$), changes in near-surface wind speed ($\frac{\overline{Q_E}}{\overline{W}}W'$), and sensible heat flux (Q_H). D_o represents the sum of zonal, meridional, and vertical advection of ocean heat transport. The residual term consists of heat transport related to unresolved processes, including diffusion, submesoscale processes, and mixing and diabatic processes (Abellán *et al* 2018). Our study concerns the SST spatial pattern formation in the tropical Atlantic for the ten-year idealized pacemaker simulations (IPO+ minus IPO−). Because all radiative forcings are kept constant at the pre-industrial levels in both models, the SST change ($\frac{\partial T}{\partial t}$) is in a quasi-equilibrium between the four surface heat flux components and ocean dynamics (D_o) (see a complete analysis of the ocean mixed-layer heat budget analysis shown in Text S1 in the supplementary information). As ocean current velocities are not currently available in the IPO idealized pacemaker simulations for some realizations of HadGEM3-GC31-MM, the presentation of our main results is centered on IPSL-CM6A-LR. Given a robust validation of the IPO-tropical Atlantic connections in both climate models, our main conclusions hold for HadGEM3-GC31-MM.

We found that the downward longwave radiation increase is the primary contributor to relaying the IPO-SST warming signal to the basin-wide SST over the tropical Atlantic (figure 4(a)), in line with earlier results (Meehl *et al* 2021). Although other surface heat flux components, including shortwave radiation, sensible heat flux, and latent heat flux, along with ocean dynamics, contribute partly to SST warming at some locations in the tropical Atlantic sector (figure S9), all of them are not sufficient to fully explain the basin-scale warming in the tropical Atlantic. More specifically, a warm-phase IPO-SST anomaly heats the tropical tropospheric atmospheric temperature aloft over the Atlantic via the eastward-propagating Kelvin wave (Yulaeva and Wallace 1994, Chiang and Sobel 2002). Moreover, the altered Walker circulation induces anomalous subsidence in the tropical Atlantic, adiabatically warming the tropospheric atmosphere. Both atmospheric processes allow the tropospheric atmosphere to hold more moisture (figure 4(b)) and increase the total cloud fraction associated with larger relative humidity (solid contours in figure 4(d)). Because atmospheric water vapor absorbs infrared radiation and is an important greenhouse gas, a larger concentration of water vapor results in higher SSTs by increasing downward longwave radiation (figure 4(a)). As SST increases, more water vapor from the warm ocean will evaporate into the overlying atmosphere, and a positive feedback mechanism between water vapor and SST is established (Chu and Murakami 2022). Thus, the tropical Atlantic widespread SST warming is dominated by the downward longwave radiation, whose contribution is larger than that due to an increase in the relative humidity-induced and atmospheric stability-related latent heat flux (figures 4(d) and (e)).

These results disagree with previous findings, which suggest that the latent heat flux and solar radiation give rise to the tropical north Atlantic warming response to ENSO on the inter-annual timescale (Curtis and Hastenrath 1995, Klein *et al* 1999, Chiang and Sobel 2002). Our study highlights that the warming effects induced by the water vapor-longwave radiation-SST positive feedback completely

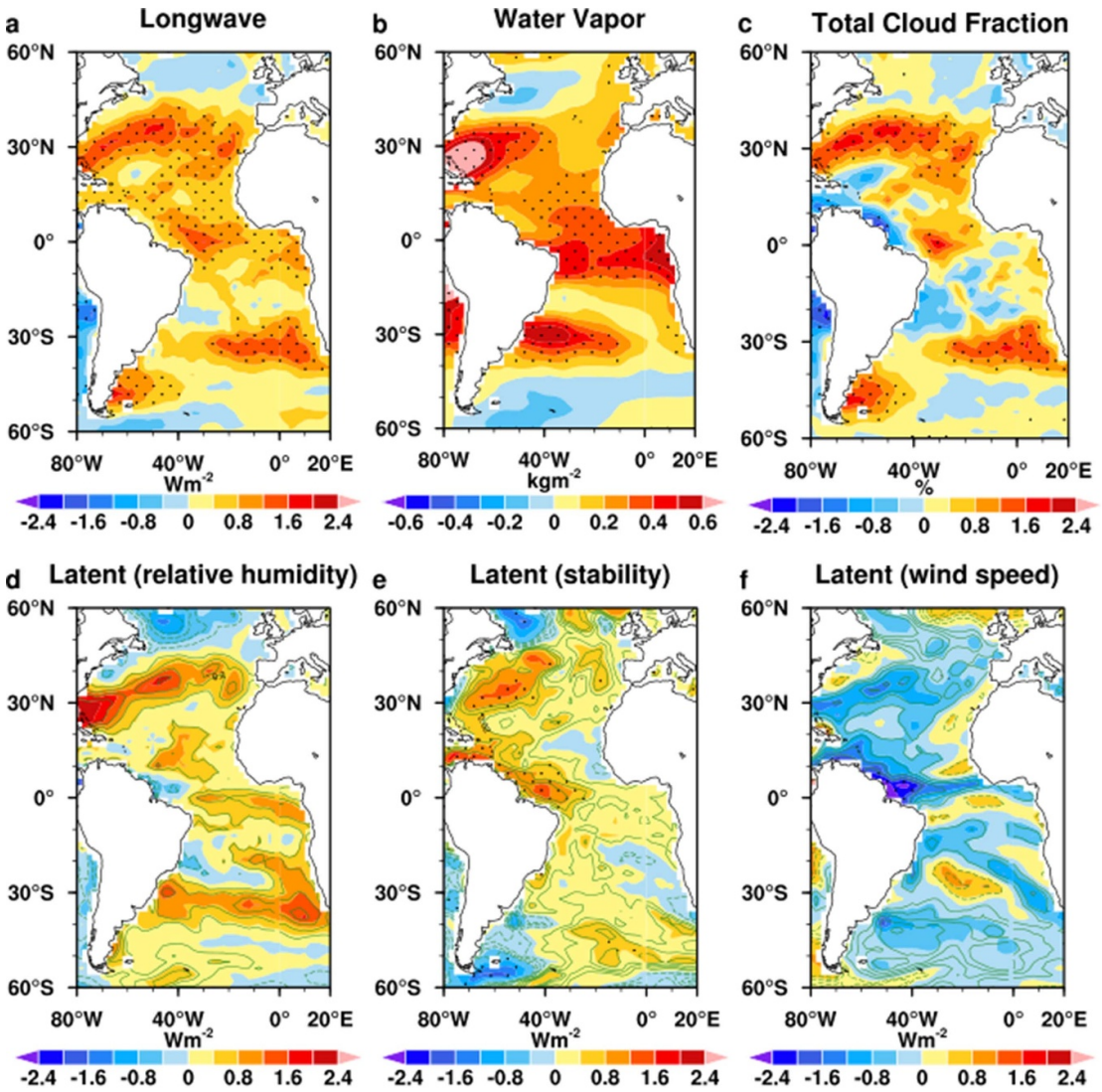

Figure 4. The physical processes for a warm-phase IPO-SST anomaly heating the tropical Atlantic in IPSL-CM6A-LR (IPO+ minus IPO−). (a) Longwave radiation, (b) atmospheric water vapor content, (c) total cloud fraction, and latent heat flux due to (d) variations in relative humidity (shading denotes relative humidity-related latent heat and contours with an interval of 0.1% from −0.4% to 0.4%; solid contours represent increased relative humidity), (e) changes in atmospheric stability (shading represents stability-related latent heat and contours with an interval of 0.01 °C from −0.04 °C to 0.04 °C; solid contours indicates enhanced air-sea temperature difference), (f) changes in near-surface wind speed (shading represents wind speed related latent heat and contours with an interval of 0.01 m s^{-1} from −0.08 m s^{-1} to 0.08 m s^{-1}; solid contours denote increased wind speed). The surface heat flux is positive downward. Stippling denotes regions exceeding 95% statistical significance based on a two-sided student *t*-test.

negate the cooling effects arising from the increased latent heat loss due to strengthened near-surface speed via both the Walker circulation weakening and mid-latitude Rossby wave response (figure 4(f)), consistent with earlier studies (Meehl *et al* 2021) indicating that the teleconnections produced the tropical Atlantic weakened easterlies and latent heat flux reduction that added to the warming effects from increased downward longwave radiation. Our results further confirm that the water vapor-longwave radiation-SST positive feedback should be mainly responsible for the decadal-timescale tropical Atlantic basin-wide warming response to a warm-phase IPO-SST anomaly.

4. Conclusion

Using a series of idealized warm-phase and cold-phase IPO pacemaker experiments with two global coupled models, we have shown that a warm-phase (cold-phase) IPO-SST anomaly drives basin-wide SST warming (cooling) response over the tropical Atlantic through both the tropical and mid-latitude atmospheric teleconnections. For a warm-polarity IPO-SST case, the tropical tropospheric atmosphere markedly warms and can thus hold more water vapor. A warmer and more damp tropospheric atmosphere causes downward longwave radiation to increase, eventually heating the basin-wide SST across

the tropical Atlantic. On the contrary, a weakened Pacific Walker circulation, in combination with the mid-latitude Rossby wave responses, amplifies the sea level pressure over the tropical Atlantic. The resultant tropical Atlantic-Pacific trans-basin pressure gradient increases and produces strengthened trade winds over the tropical Atlantic, especially in IPSL-CM6A-LR, contrary to HadGEM3-GC31-MM and CESM1 (Meehl *et al* 2021). The trade wind intensification seems to cool the tropical Atlantic SST via the Bjerknes positive feedback mechanism. Accordingly, the large-scale warming in the tropical Atlantic, as a consequence of a warm-phase IPO-SST forcing, is dominated by the tropospheric atmospheric temperature mechanism that overwhelmingly counterbalances the atmospheric bridge mechanism comprising a reduced Pacific Walker circulation and the mid-latitude Rossby wave responses.

A possible caveat is that the IPO-tropical Atlantic decadal teleconnections may be model-dependent. Notably, the tropical Atlantic trade winds depend more on the geographic pattern of mid-latitude teleconnections. For IPSL-CM6A-LR, anomalous low-pressure centers of action in the extra-tropical North and South Atlantic reside near 50°N and 65°S (figure 3(e)), too farther poleward to impact the tropical Atlantic trade winds, leading to the prevailing easterlies between 20°N and 20°S (figure 1(a)). By comparison, anomalous low-pressure active centers dwell near 30°N and 50°S in HadGEM3-GC31-MM (figure 3(f)) and CESM1 (Meehl *et al* 2021), and comparatively, weak trade winds appear only along the equatorial Atlantic (figure 1(b)). Overall, large increases in downward longwave radiation effectively negate latent heat flux loss related to the strengthened trade winds, eventually leading to a basin-wide SST warming over the tropical Atlantic. The three coupled model results reflect a physical consistency of the tropical Atlantic basin-scale warming response to a warm-polarity IPO-SST forcing.

Our results suggest that an IPO-SST anomaly creates a same-sign SST response in the tropical Atlantic. However, the converse is not the case. Previous studies have documented that the Atlantic SST rapid warming during a warm-polarity Atlantic Multi-decadal Variability (AMV) amplifies cold SST anomalies over the eastern-central tropical Pacific (Kucharski *et al* 2011, McGregor *et al* 2014, Li *et al* 2016, Ruprich-Robert *et al* 2017, Meehl *et al* 2021, Yao *et al* 2021). On the other hand, recent modeling studies argue that while the IPO mostly originates from internal variability, external forcings contribute to the tropical Pacific decadal SST variations since the 1990s, and anthropogenic aerosols have modulated the magnitude of a cold-phase IPO-SST anomaly since 1998 (Hua *et al* 2018). The AMV is, instead, a consequence of the combination of internal variability and volcanic and anthropogenic aerosols (Qin *et al* 2020a, 2020b). Thus, it remains challenging to determine what leads the IPO to change phase and what causes the AMV itself to shift phase. However, at least to a certain degree, we realize that the Pacific and Atlantic could be mutually interactive on the decadal timescale (e.g. about ten years), with one alternatively impacting another (Meehl *et al* 2021). A broader understanding of the decadal-scale trans-basin Pacific-Atlantic climate interactions may provide a physical basis for improving decadal predictions of global warming rates, considering emerging evidence that the net impact of multiple ocean basin SST changes contributes to the global warming acceleration and slowdown (Drijfhout *et al* 2014, Yao *et al* 2017).

Data availability statement

All the model data presented in our study are publicly available at https://catalogue.ceda.acuk/uuid/4bf2f8d1dfd6470ba783f36bc9f581b3?jump=related-anchor

Acknowledgments

We thank Dr Gerald Meehl and an anonymous reviewer for helpful comments that significantly improved this study. This work was supported by the National Youth Fund Program of China (42005134) and the Chinese Postdoctoral Innovative Talent Program (119100582Q). F Z was supported by the National Natural Science Foundation of China (41790474), the National Key Research and Develpment Project (2018YFA0606404), and the National Key R&D Program of China (2020YFA0608902). We acknowledge the World Climate Research Programme's working group on coupled modeling for providing model datasets. Thanks to May Izumi for her assistance in editing our writing.

Conflict of interest

The authors declare no competing interests.

References

Abellán E, McGregor S, England M H and Santoso A 2018 Distinctive role of ocean advection anomalies in the development of the extreme 2015–16 El Niño *Clim. Dyn.* **51** 2191–208

Bjerknes J 1969 Atmospheric teleconnections from the equatorial Pacific *Mon. Weather Rev.* **97** 163–72

Boer G J *et al* 2016 The decadal climate prediction project (DCPP) contribution to CMIP6 *Geosci. Model Dev.* **9** 3751–77

Boucher O *et al* 2020 Presentation and evaluation of the IPSL-CM6A-LR climate model *J. Adv. Model. Earth Syst.* **12** e2019MS002010

Cai W *et al* 2019 Pantropical climate interactions *Science* **363** eaav4236

Chang P *et al* 2006b Climate fluctuations of tropical coupled systems—the role of ocean dynamics *J. Clim.* **19** 5122–74

Chang P, Fang Y, Saravanan R, Ji L and Seidel H 2006a The cause of the fragile relationship between the Pacific El Niño and the Atlantic Niño *Nature* **443** 324–8
Chang P, Saravanan R, Ji L and Hegerl G C 2000 The effect of local sea surface temperatures on atmospheric circulation over the tropical Atlantic sector *J. Clim.* **13** 2195–216
Chiang J C and Sobel A H 2002 Tropical tropospheric temperature variations caused by ENSO and their influence on the remote tropical climate *J. Clim.* **15** 2616–31
Chu P-S and Murakami H 2022 *Climate Variability and Tropical Cyclone Activity* (Cambridge: Cambridge University Press)
Curtis S and Hastenrath S 1995 Forcing of anomalous sea surface temperature evolution in the tropical Atlantic during Pacific warm events *J. Geophys. Res. Oceans* **100** 15835–47
Deser C, Phillips A S and Hurrell J W 2004 Pacific interdecadal climate variability: linkages between the tropics and the North Pacific during boreal winter since 1900 *J. Clim.* **17** 3109–24
Drijfhout S S, Blaker A T, Josey S A, Nurser A, Sinha B and Balmaseda M 2014 Surface warming hiatus caused by increased heat uptake across multiple ocean basins *Geophys. Res. Lett.* **41** 7868–74
Frankignoul C and Kestenare E 2002 The surface heat flux feedback. Part I: estimates from observations in the Atlantic and the North Pacific *Clim. Dyn.* **19** 633–47
Gill A E 1980 Some simple solutions for heat-induced tropical circulation *Q. J. R. Meteorol. Soc.* **106** 447–62
Grimm A M and Tedeschi R G 2009 ENSO and extreme rainfall events in South America *J. Clim.* **22** 1589–609
Ham Y-G, Kug J-S, Park J-Y and Jin F-F 2013 Sea surface temperature in the north tropical Atlantic as a trigger for El Niño/Southern Oscillation events *Nat. Geosci.* **6** 112–6
Han W *et al* 2014 Intensification of decadal and multi-decadal sea level variability in the western tropical Pacific during recent decades *Clim. Dyn.* **43** 1357–79
Haney R L 1971 Surface thermal boundary condition for ocean circulation models *J. Phys. Oceanogr.* **1** 241–8
Hastenrath S and Heller L 1977 Dynamics of climatic hazards in northeast Brazil *Q. J. R. Meteorol. Soc.* **103** 77–92
Hua W, Dai A and Qin M 2018 Contributions of internal variability and external forcing to the recent Pacific decadal variations *Geophys. Res. Lett.* **45** 7084–92
Klein S A, Soden B J and Lau N-C 1999 Remote sea surface temperature variations during ENSO: evidence for a tropical atmospheric bridge *J. Clim.* **12** 917–32
Kosaka Y and Xie S-P 2013 Recent global-warming hiatus tied to equatorial Pacific surface cooling *Nature* **501** 403–7
Kucharski F, Kang I S, Farneti R and Feudale L 2011 Tropical Pacific response to 20th century Atlantic warming *Geophys. Res. Lett.* **38** L03702
Kumar A and Hoerling M P 2003 The nature and causes for the delayed atmospheric response to El Niño *J. Clim.* **16** 1391–403
Latif M 2001 Tropical Pacific/Atlantic Ocean interactions at multi-decadal time scales *Geophys. Res. Lett.* **28** 539–42
Li X *et al* 2021 Tropical teleconnection impacts on Antarctic climate changes *Nat. Rev. Earth Environ.* **2** 680–98
Li X, Holland D M, Gerber E P and Yoo C 2014 Impacts of the north and tropical Atlantic Ocean on the Antarctic Peninsula and sea ice *Nature* **505** 538–42
Li X, Xie S-P, Gille S T and Yoo C 2016 Atlantic-induced pan-tropical climate change over the past three decades *Nat. Clim. Change* **6** 275–9
McGregor S, Timmermann A, Stuecker M F, England M H, Merrifield M, Jin F-F and Chikamoto Y 2014 Recent Walker circulation strengthening and Pacific cooling amplified by Atlantic warming *Nat. Clim. Change* **4** 888–92
Meehl G A, Hu A, Castruccio F, England M H, Bates S C, Danabasoglu G, McGregor S, Arblaster J M, Xie S-P and Rosenbloom N 2021 Atlantic and Pacific tropics connected by mutually interactive decadal-timescale processes *Nat. Geosci.* **14** 36–42
Meehl G A, Hu A, Santer B D and Xie S-P 2016 Contribution of the Interdecadal Pacific Oscillation to twentieth-century global surface temperature trends *Nat. Clim. Change* **6** 1005–8
Mo K C 2000 Relationships between low-frequency variability in the southern hemisphere and sea surface temperature anomalies *J. Clim.* **13** 3599–610
Newman M *et al* 2016 The Pacific Decadal Oscillation, revisited *J. Clim.* **29** 4399–427
Nigam S, Sengupta A and Ruiz-Barradas A 2020 Atlantic–Pacific links in observed multidecadal SST variability: is the Atlantic multidecadal oscillation's phase reversal orchestrated by the Pacific Decadal Oscillation? *J. Clim.* **33** 5479–505
Pan Y H and Oort A H 1983 Global climate variations connected with sea surface temperature anomalies in the eastern equatorial Pacific Ocean for the 1958–73 period *Mon. Weather Rev.* **111** 1244–58
Power S, Casey T, Folland C, Colman A and Mehta V 1999 Inter-decadal modulation of the impact of ENSO on Australia *Clim. Dyn.* **15** 319–24
Qin M, Dai A and Hua W 2020a Quantifying contributions of internal variability and external forcing to Atlantic multidecadal variability since 1870 *Geophys. Res. Lett.* **47** e2020GL089504
Qin M, Dai A and Hua W 2020b Aerosol-forced multidecadal variations across all ocean basins in models and observations since 1920 *Sci. Adv.* **6** eabb0425
Roberts M J *et al* 2019 Description of the resolution hierarchy of the global coupled HadGEM3-GC3. 1 model as used in CMIP6 HighResMIP experiments *Geosci. Model Dev.* **12** 4999–5028
Ruprich-Robert Y, Msadek R, Castruccio F, Yeager S, Delworth T and Danabasoglu G 2017 Assessing the climate impacts of the observed Atlantic multidecadal variability using the GFDL CM2. 1 and NCAR CESM1 global coupled models *J. Clim.* **30** 2785–810
Sasaki W, Richards K J and Masumoto Y 2015 The influence of ENSO on the equatorial Atlantic precipitation through the Walker circulation in a CGCM *Clim. Dyn.* **44** 191–202
Servonnat J, Mignot J, Guilyardi E, Swingedouw D, Séférian R and Labetoulle S 2015 Reconstructing the subsurface ocean decadal variability using surface nudging in a perfect model framework *Clim. Dyn.* **44** 315–38
Soden B J 2000 The sensitivity of the tropical hydrological cycle to ENSO *J. Clim.* **13** 538–49
Takaya K and Nakamura H 2001 A formulation of a phase-independent wave-activity flux for stationary and migratory quasigeostrophic eddies on a zonally varying basic flow *J. Atmos. Sci.* **58** 608–27
Taschetto A S, Rodrigues R R, Meehl G A, McGregor S and England M H 2016 How sensitive are the Pacific–tropical North Atlantic teleconnections to the position and intensity of El Niño-related warming? *Clim. Dyn.* **46** 1841–60
Ting M, Kushnir Y, Seager R and Li C 2009 Forced and internal twentieth-century SST trends in the North Atlantic *J. Clim.* **22** 1469–81
Wallace J M and Gutzler D S 1981 Teleconnections in the geopotential height field during the northern hemisphere winter *Mon. Weather Rev.* **109** 784–812
Xie L, Yan T, Pietrafesa L J, Morrison J M and Karl T 2005 Climatology and interannual variability of North Atlantic hurricane tracks *J. Clim.* **18** 5370–81
Xie S-P, Deser C, Vecchi G A, Ma J, Teng H and Wittenberg A T 2010 Global warming pattern formation: sea surface temperature and rainfall *J. Clim.* **23** 966–86
Yao S L, Zhou W, Jin F F and Zheng F 2021 North Atlantic as a trigger for Pacific-wide decadal climate change *Geophys. Res. Lett.* **48** e2021GL094719
Yao S-L, Luo J-J, Huang G and Wang P 2017 Distinct global warming rates tied to multiple ocean surface temperature changes *Nat. Clim. Change* **7** 486–91

Yu J-Y, Kao H-Y and Lee T 2010 Subtropics-related interannual sea surface temperature variability in the central equatorial Pacific *J. Clim.* **23** 2869–84
Yulaeva E and Wallace J M 1994 The signature of ENSO in global temperature and precipitation fields derived from the microwave sounding unit *J. Clim.* **7** 1719–36
Zhang Y, Wallace J M and Battisti D S 1997 ENSO-like interdecadal variability: 1900–93 *J. Clim.* **10** 1004–20